Analytical Management of SCR Catalyst Lifetimes and Multipollutant Performance

Paper No. 22

Stephen Niksa and Balaji Krishnakumar
Niksa Energy Associates LLC, 1745 Terrace Drive, Belmont, CA 94002

Farrokh Ghoreishi and Corey Tyree
Southern Company Services, Inc., 600 N. 18th St., Birmingham, AL 35203

ABSTRACT

SCR catalysts are deactivated by several mineral and metallic trace elements at highly variable rates determined by fuel quality and furnace firing conditions. With a loss in activity, NO is reduced over a longer inlet length of the SCR monolith, which leaves a shorter trailing section to sustain the most favorable conditions to oxidize Hg^0 and SO_2. Since no operating SCR was designed for Hg oxidation and since different monoliths have been combined as layers in particular units, the Hg oxidation performance of any particular SCR fleet is largely unmanaged. The analysis in this paper directly relates a measurement or manufacturers forecast on the deterioration in NO reduction with age to corresponding estimates for oxidation of Hg^0. It accommodates any number of catalyst layers with grossly different properties including materials from different manufacturers, and different ages. In this paper, the analysis is applied to 16 full-scale SCRs in the Southern Company fleet to determine which SCRs can meet targets on Hg^0 oxidation performance given the current age, and which may need an additional layer in the near future.

INTRODUCTION

Selective Catalytic Reduction (SCR) technology has become the technology of choice to meet stringent NO_X emissions limits for coal-fired power plants. Along with NO reduction, SCR units also sustain Hg oxidation. The oxidation of elemental Hg (Hg^0) into oxidized Hg (Hg^{2+}) is important because only Hg^{2+} is water soluble and therefore amenable to capture in FGD scrubbing solutions. Extents of Hg^0 oxidation of 90 % or more are routinely recorded in full-scale field tests,[1] provided that the flue gas contains abundant Cl- or Br-species and that the SCR provides sufficient reactivity, favorable mass transport rates, and ample residence time for the chemistry to proceed to near-completion. When these conditions are satisfied, SCR/ESP/FGD combinations are also the technology of choice for Hg control because they require no special reagents or

1

operating procedures to lower Hg emissions. Unfortunately, SCR catalysts also oxidize SO_2 into SO_3, and elevated SO_3 levels can significantly exacerbate plume opacity problems once the SO_3 condenses into fumes in the air preheater and beyond.

This paper demonstrates an analytical strategy to actively manage the multipollutant performance of an entire fleet of full-scale SCRs and its deterioration in time due to catalyst deactivation. The underlying performance model was introduced previously,[2] and validated with extensive datasets on catalysts from four of the most popular SCR vendors in the American industry.[3,4] It simultaneously describes the conversion of NO, Hg^0 and SO_2 along SCR catalyst channels in terms of the rates of film transport from the free stream to the external surface of a catalyst channel; diffusion of reactants through the internal catalyst pores; and the chemical conversion of the adsorbed participating species. In this study, the catalyst channel model was expanded into a simulator for full-scale SCRs in which the properties of each layer in the monolith are completely independent, so that layers can have different geometrical specifications and ages, and come from different vendors. We also incorporated the manufacturers' activity ratios for NO reduction to describe how the NO reduction performance deteriorates with age. Two limiting scenarios were developed to relate the deactivation of the activities for NO reduction and Hg^0 oxidation: one where they are proportional and another in which only NO reduction is deactivated which indirectly affects Hg^0 oxidation.

The SCR simulations were applied to 16 full-scale SCRs in the Southern Company (SC) fleet to rank order the Hg^0 oxidation performance. Pending a satisfactory validation of the predictions, the analysis will enable regional plant managers to direct their resources toward the units that can deliver the best benefits, and to identify the most favorable strategies for the allocation of new catalysts within a particular SCR.

SCR UNIT SIMULATIONS

Simulations for full-scale, multilayer SCR monoliths were developed from a package with three primary elements: (1) The SCR Catalyst Model, which describes the multipollutant performance along individual catalyst channels; (2) A calculation sequence that evaluates the SCR Catalyst Model in series for the properties of each successive catalyst layer in the monolith; and (3) A catalyst deactivation algorithm, which reduces the reactivities for NO reduction and, perhaps, Hg^0 oxidation according to a manufacturer's activity at a specified age and the actual age of each catalyst layer. This section describes each element in turn.

The SCR Catalyst Model

NEA introduced the first reaction mechanism for simultaneous NO reduction and Hg^0oxidation in terms of lumped catalyst reactivities that resolved film transport of reactants onto the external catalyst channel wall from an overall chemical reactivity.[5] The key features were a competition between NH_3 and HCl for surface sites, and an Hg^0 oxidation reaction on the chlorinated catalyst sites. This competitive adsorption subdivides the catalyst into two stages. An entry stage sustains NO reduction with high

concentrations of adsorbed NH_3 but the population of chlorinated sites remains very small as long as the HCl concentration is much lower than the NH_3 concentration. This small population oxidizes relatively small proportions of the Hg^0. Once the NH_3 has been consumed, a trailing stage is chlorinated much more extensively and therefore able to rapidly oxidize Hg^0. This mechanism interpreted extents of Hg^0 oxidation by Cl species in lab-, pilot-, and full-scale SCR units for the complete domain of utility gas cleaning conditions. The strong coupling between NO reduction and Hg^0 oxidation via competitive adsorption of NH_3 and HCl was also independently validated with an extensive series of lab tests.[6]

Additional modeling work[2] expanded the original lumped analysis in two ways. First, simultaneous SO_2 oxidation was incorporated and, second, the analysis now resolves internal pore diffusion across the catalyst wall thickness from the intrinsic reactivity of adsorbed species on the catalyst surface with a conventional Thiele analysis, to directly relate catalyst morphology and composition to the multipollutant performance of the SCR reactor. NEA's original mechanism for catalytic Hg^0 oxidation has been incorporated into this framework to account for the mediation of competitive HCl and NH_3 adsorption by pore diffusion. A simple premise connects NO and SO_2 conversion to the Hg^0 oxidation behavior on SCRs: That HCl competes for surface sites with NH_3, and that Hg^0 contacts these chlorinated sites either from the gas phase or as a weakly adsorbed species.

The various reactivities and the parameters in numerous adsorption equilibrium relations were specified to quantitatively match the reported extents of Hg^0 oxidation across broad domains of gas cleaning conditions (halogen levels, NH_3/NO ratios, space velocities, temperatures) for catalysts from four major vendors at both the pilot- and full-scale[3,4]. None of these parameters were adjusted in the present study.

The Calculation Sequence

In the simulations, the design specifications and age for each catalyst layer in the monolith are completely independent, so SCR monoliths may be constructed with layers from different manufacturers; with honeycomb or plate catalysts; with different geometrical specifications; and with different ages in each layer, as usually found in full-scale SCRs in service. The flue gas composition is specified at the SCR inlet, and then evaluated as a function of distance across each layer throughout the monolith.

In the calculation sequence, an early calculation loop uses the coal properties to assign a complete flue gas composition by varying the air flowrate to match the estimated flue gas O_2 concentration to a reported value. The governing equations are then solved to determine extents of NO reduction, SO_2 oxidation, and Hg^0 oxidation along the multiple catalyst layers by accounting for their deactivation, according to the procedure outlined in the next subsection. The expanded analysis re-starts the boundary layer growth at the inlet to each layer, which is important because mass-transfer coefficients are nominally infinite at the inlet to every layer. Even though the coefficients rapidly decay as the boundary layer develops, the enhanced mass transfer at the layer inlets definitely boosts the performance of the whole SCR, and these enhancements are now imposed at the

beginning of every layer. Among the important factors that determine SCR performance, the only one that is not included is flue gas maldistribution. Each simulation takes less than 5 s on a dual-core microprocessor operating at 1.86 GHz.

We characterize the extent of Hg conversion across an SCR with the extent of Hg^0 oxidation, $^{SCR}X_{Hg0}$, which is defined as follows:

$$^{SCR}X_{Hg^0} = 100 \frac{^{IN}C_{Hg^0} - ^{OUT}C_{Hg^0}}{^{IN}C_{Hg^0}}$$ (1)

where C_{Hg0} represents the Hg^0 concentrations at the inlet and outlet of the SCR monolith. The analogous conversion across a particular layer is denoted at $^{1}X_{Hg0}$.

Catalyst Deactivation Protocol

Deactivation histories estimated by the manufacturer were provided for every catalyst layer in this study in the form of the initial NO reduction activity of the fresh catalyst (k_0 in m/h) and the activity at the end of 16,000 hours of operation (k_M). Catalyst manufacturers generally account for the ash loading of the primary coal feedstock in specifying the deactivation history but whether they account for the expected poisons from each coal type or not is unknown. We used the reported operating hours for each layer and the manufacturer's deactivation history to estimate the residual activity for age t in terms of the activity ratio, k_d/k_0, which is the ratio of the catalyst activity at any time, k_d, to the initial catalyst activity, k_0. This estimate is given by the following formula:

$$\frac{k_d}{k_0} = \frac{\frac{k_M}{k_0} - 1}{t_M} t + 1$$ (2)

Where t_M is 16,000 h and t is the actual operating hours for the subject catalyst layer. For the oldest layers, this linear extrapolation gave very low or even negative residual activities, so the minimum activity ratio was fixed at 0.4.

Several gaseous species of As, P, K, Na, Cd, Pb, Cu and others have been identified in the literature as poisons for SCR catalysts. In addition, solid compounds such as gypsum, ammonium bisulfate and aerosol salts of Na, K and other alkaline earth metals deactivate SCR catalysts by fouling and pore blocking. Aerosol salts of Ca and to a lesser extent Na and K generally block the catalyst pores and prevent the adsorption of NH_3 and HCl while oxides of As and P react with surface V−OH and V=O sites and deactivate them. Whereas deactivation mechanisms like pore blocking will affect both NH_3 and HCl adsorption and, consequently, NO reduction and Hg^0 oxidation, chemical deactivation will definitely affect NO reduction but not necessarily Hg^0 oxidation. Unfortunately enough information is not available in the literature to examine the exact conditions and the contribution of each SCR catalyst deactivation mechanism to the deactivation of Hg^0 oxidation. Consequently, we implement the deactivation of Hg^0 oxidation across the SCR in two limiting scenarios that bound the tendencies for the deactivation by pore blocking alone and by simultaneous pore blocking and chemical deactivation.

4

Our first deactivation approach is for situations where pore blockage comes into play where the deactivation mechanisms prevent the active sites on the catalyst from reacting with both NH_3/NO and HCl/Hg^0 species, hereinafter referred to as 'Type I' deactivation. Such deactivation excludes sites from participating in both reactions, and thereby diminishes the site population. Smaller site populations necessarily support smaller surface coverages of NH_3 and Cl adsorbate species that are required for NO reduction and Hg^0 oxidation, respectively. To account for the decreased coverages, we decrease the reactivities of both NO reduction and Hg^0 oxidation by a common multiplicative factor, because the reactivities in our rate expressions implicitly include the total population of active sites on the catalyst as a multiplicative factor. The deactivation factor is specified to match the lower extent of NO reduction for the deactivated catalyst, which is given by

$$^I X_{NO,d} = \alpha \left[1 - (1 - \frac{^I X_{NO,0}}{\alpha})^{\frac{k_d}{k_0}} \right]$$

(3)

where α is the NH_3/NO ratio at the inlet; $^I X_{NO,0}$ is the reference NO conversion across layer I for fresh catalyst; and $^I X_{NO,d}$ is the estimate for NO reduction across the deactivated layer. Then the reactivity for NO reduction in the SCR Catalyst Model is adjusted to give a predicted NO reduction across the layer of $^I X_{NO,d}$. The same percentage adjustment is applied to the reactivity for Hg^0 oxidation. The resulting reduction in Hg^0 oxidation is a direct consequence of the lower Hg oxidation reactivity compounded by increased inhibition due to a greater concentration of NH_3 further into the layer. Note that deactivation of NO reduction always sustains a greater NH_3 concentration deeper into any catalyst layer, and greater NH_3 concentrations inhibit Hg^0 oxidation more strongly. Such compounding is important for Type I deactivation, but not for Type II deactivation.

The second deactivation scenario addresses the situations where mechanisms prevent the active sites on the catalyst from reacting with NH_3/NO but not with HCl/Hg^0 species, hereinafter referred to as 'Type II' deactivation. The second type is implemented in the same way as the first, except that only the NO reactivity is progressively lowered to match the value of $^I X_{NO,d}$ for the estimated activity ratio, instead of lowering the reactivities for both NO reduction and Hg^0 oxidation. Even though both deactivation scenarios are calibrated to the same $^I X_{NO,d}$, Type II deactivation exerts a weaker impact on Hg^0 oxidation, because stronger NH_3 inhibition is the only effect that comes into play. With Type I deactivation, Hg^0 oxidation is diminished by the direct reduction in the Hg^0 oxidation reactivity plus the stronger inhibition associated with the greater NH_3 concentrations resulting from the lower reactivity for NO reduction. With Type II deactivation, there is no direct reduction in the Hg^0 oxidation reactivity, so extents of Hg^0 oxidation are diminished exclusively by the stronger NH_3 inhibition for the lower NO reduction reactivity, which persists along a greater length of the monolith.

SUBJECT SCR FLEET

Our simulations use detailed design specifications for sixteen full-scale SCRs at nine power plants, seven of which fire bituminous coals and two fire PRB subbituminous

Figure 1. Predicted profiles of NH_3 and NO concentrations (left y-axes), and cumulative NO and Hg^0 conversions (right y-axes) across (left panel) fresh catalyst and (right panel) in-service catalysts whose ages varied by a factor of two.
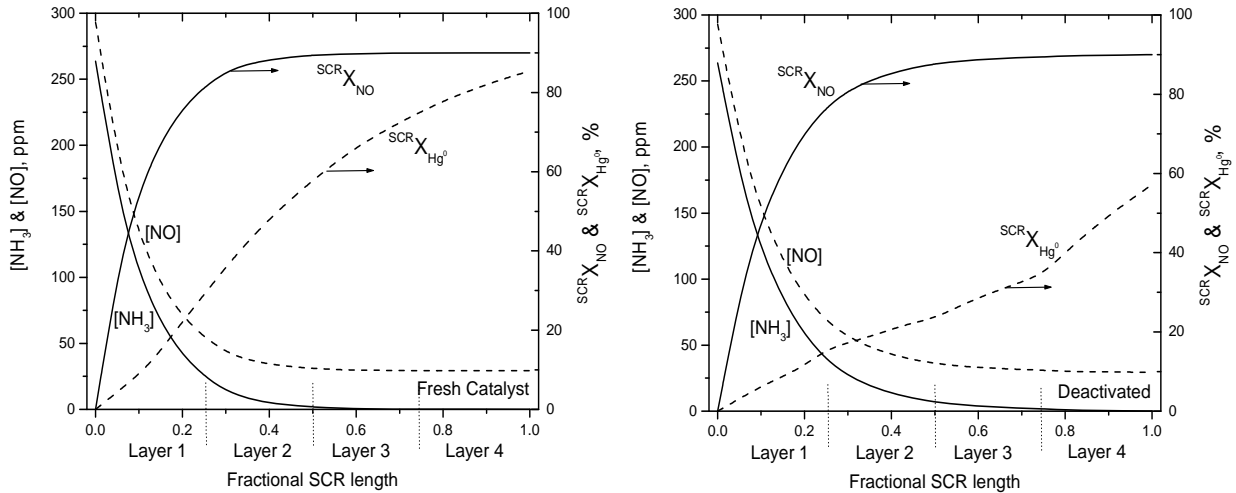
coals. The flue gas HCl concentrations varied from 4 to 99 ppmv, and inlet NO concentrations ranged from 92 to 457 ppm. The gas hourly space velocities (GHSV) varied between 1424 and 3076 h^{-1}. Most SCRs operated between 370 and 405°C although this variation would only affect Hg^0 oxidation in the hottest units. Most of the SCRs had four catalyst layers, some has three, while only one has two layers. Most of the catalyst layers were honeycombs, although there were also plate monoliths from different vendors. The ages of the catalyst layers varied from 4,000 to 51,000 h, which correspond to activity ratios from 0.4 to 0.94.

SIMULATION RESULTS

We first illustrate the most important features of deactivation across multilayer monoliths with simulations for an SCR with four honeycomb layers with identical design characteristics but ages that varied by a factor of two. The flue gas was generated with an Eastern bituminous coal. In simulations for the left panel of Fig. 1, all catalysts were fresh and therefore had an activity ratio of unity. The predicted axial profiles for NH_3 and NO concentrations and NO and Hg^0 conversions are plotted along a normalized length coordinate where '0.0' represents the entrance to the first layer and '1.0'represents the exit from the last layer. Since all four layers installed in this SCR are physically identical, a length increment of 0.25 represents the length of each catalyst layer. The interlayer distances are not shown.

The NO and NH_3 concentrations drop sharply in the first layer with a corresponding increase in $^{SCR}X_{NO}$ such that at the exit of the first layer, 81.5 % NO reduction is achieved. The NO and NH_3 concentration curves exhibit similar slopes for most of the

6

SCR length with elimination of NH_3 near the outlet of the second layer. NO reduction proceeds further in the next layer although at a slower rate and quickly reaches the final asymptotic value. The remaining two layers provide minimal improvements to the NO reduction efficiency. The inhibitory effect of NH_3 on Hg^0 oxidation is also clearly observed in these figures. At the inlet of the first catalyst layer, where the NH_3 concentration is greatest, only 11 % Hg^0 is oxidized whereas 62 % of the NO has already been reduced. At the end of the first layer, Hg^0 oxidation is just below 30 % whereas NO reduction exceeds 81 %. Once NH_3 is depleted by the end of the first layer, Hg^0 oxidation is determined by the HCl concentration, which remains constant because Hg^0 conversion is too small in absolute concentration terms to affect the Cl concentration. Consequently, the extents of Hg^0 oxidation across each of the remaining layers are the same at approximately 40 % for this case, and the cumulative conversion of Hg^0 steadily increases to about 85 %. While it appears that fresh catalyst is overdesigned for NO reduction, a similar asymptotic behavior is not apparent for $^{SCR}X_{Hg0}$ due to the high HCl concentration for this case.

The impact of Type I deactivation, which is the stronger of the two deactivation types, is evident in the right panel of Fig. 1. The most reactive layers are at the two ends while catalysts with diminished activity are in the middle. Deactivation has shifted the NH_3 and NO profiles towards the right such that, at the end of the first layer, 77 % NO reduction is achieved v. 81.5 % for the fresh catalyst. This difference is not great because the first catalyst layer was relatively fresh. This relatively small difference in NO reduction is nevertheless sufficient to cut Hg^0 oxidation in half, to about 16 % from 29 % for fresh catalyst. This large difference is due to the compounding effect of the reduction in the reactivities for both NO and Hg^0 conversion. While the reduction in Hg^0 reactivity directly decreases the extent of Hg^0 oxidation, the reduction in NO reactivity allows a greater NH_3 concentration to penetrate further into the monolith. NH_3 concentrations at the exit of the first layer are 38 ppm for deactivated catalyst vs. 25 ppm for fresh catalyst. More NH_3 inhibits the adsorption of HCl and thereby diminishes Hg^0 oxidation.

Since the SCR is overdesigned for NO reduction, $^{SCR}X_{NO}$ reaches its asymptotic value towards the end of the third layer, despite strong deactivation in the second and third layers, and the simulations satisfy the threshold on NH_3 slip. In contrast, Hg^0 oxidation does not approach the constant values seen for the fresh catalyst until the final layer, which is relatively fresh, but the ultimate $^{SCR}X_{Hg0}$ is still well below the performance of the fresh monolith. The Hg^0 oxidation across the four layers was approximately 16, 9, 15 and 35 %, respectively, amounting to $^{SCR}X_{Hg0}$ of 57 % vs. about 85 % for the fresh catalyst. Also, the ages of layers 1 and 4 are identical, yet the first layer oxidized only 16 % Hg^0 whereas the fourth layer converted 35 %, clearly demonstrating the strong inhibitory effect of NH_3 in the first layer. Moreover, the $^IX_{Hg0}$ varies significantly across the different layers, which clearly demonstrates the need to account for layer-specific ages and activity ratios to obtain reasonably accurate predictions for Hg^0 oxidation.

The cumulative NO reduction and Hg^0 oxidation profiles for fresh catalyst ($^{SCR}X_{Hg0,0}$), Type I deactivation ($^{SCR}X_{Hg0,dI}$) and Type II deactivation ($^{SCR}X_{Hg0,\,dII}$) are compared in Fig. 2. As explained before, while the NO reduction efficiencies at the SCR exit for the

Figure 2. Predicted NO and Hg^0 conversion profiles across the fresh ($^{SCR}X_{NO,0}$, $^{SCR}X_{Hg0,0}$) and deactivated ($^{SCR}X_{NO,d}$, $^{SCR}X_{Hg0,dI}$, $^{SCR}X_{Hg0,dII}$) catalyst layers of the baseline SCR.
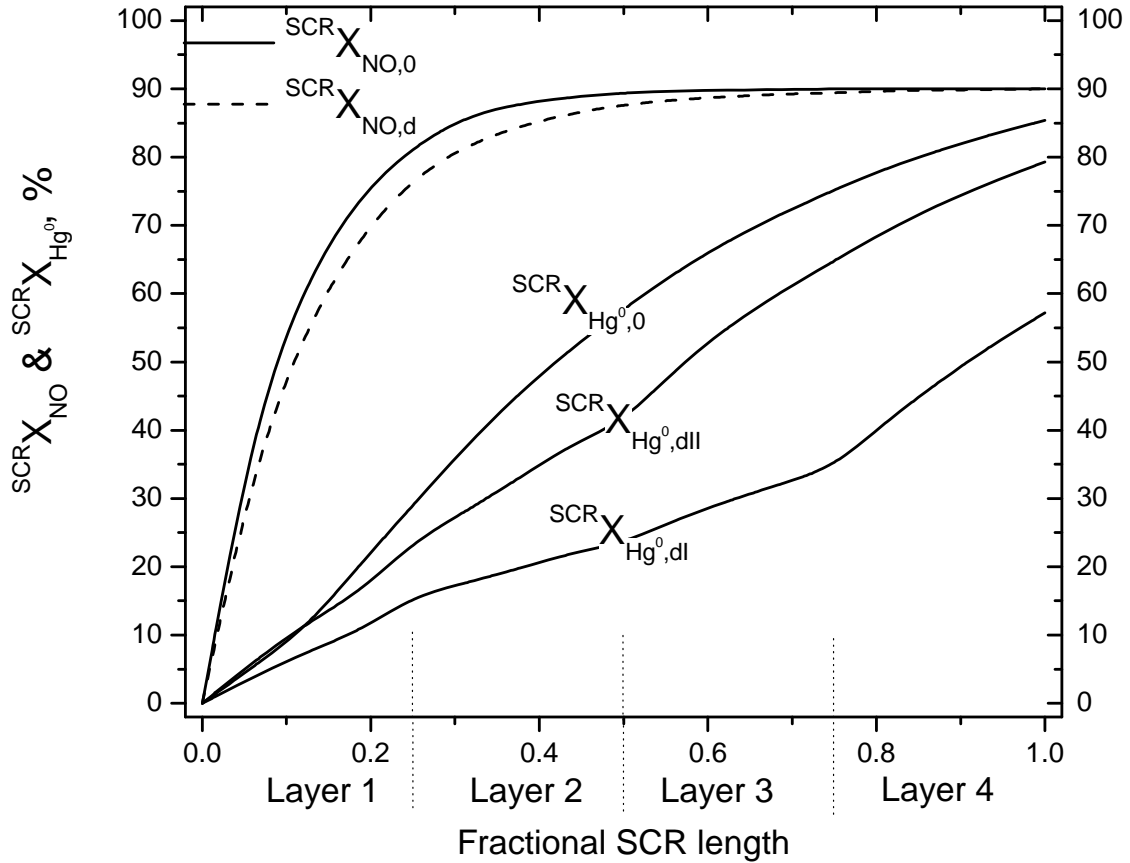
fresh and the deactivated catalysts are the same due to the overdesign of the SCR with respect to NO reduction, the $^{SCR}X_{Hg0}$ values are 85.4 % for fresh catalyst, and 57 and 79 % for deactivation of Types I and II, respectively. The substantial difference for these two deactivation scenarios highlights the importance of understanding the different catalyst poisons and their associated deactivation mechanisms.

We next consider four SCRs at the baseline power plant with four honeycomb layers of very similar design specifications, but ages that range from several thousand hours to several tens of thousands of hours. Figure 3 compares the cumulative extents of Hg^0 oxidation for Type I deactivation of these four units. The cumulative $^{SCR}X_{Hg0}$–values for the Type I deactivated catalysts, in descending order, are 57 % at Unit 1, 51 % at Unit 2, 44 % at Unit 4, and 28 % at Unit 3. This order corresponds to the sums of the operating hours of all layers in these units, which varied by a factor of two. In Fig. 3, the order at the outlet is not the same as the orders at the outlets of each layer, because the ages of any particular layer are variable. For example, across the fourth layer at Unit 2, $^{1}X_{Hg0}$ increases from 18 to 51 %, because this is the youngest layer of all, and also because NH_3

Figure 3. Predicted Hg^0 oxidation profiles across the Type I deactivated SCR catalysts for the four units at the baseline power plant.
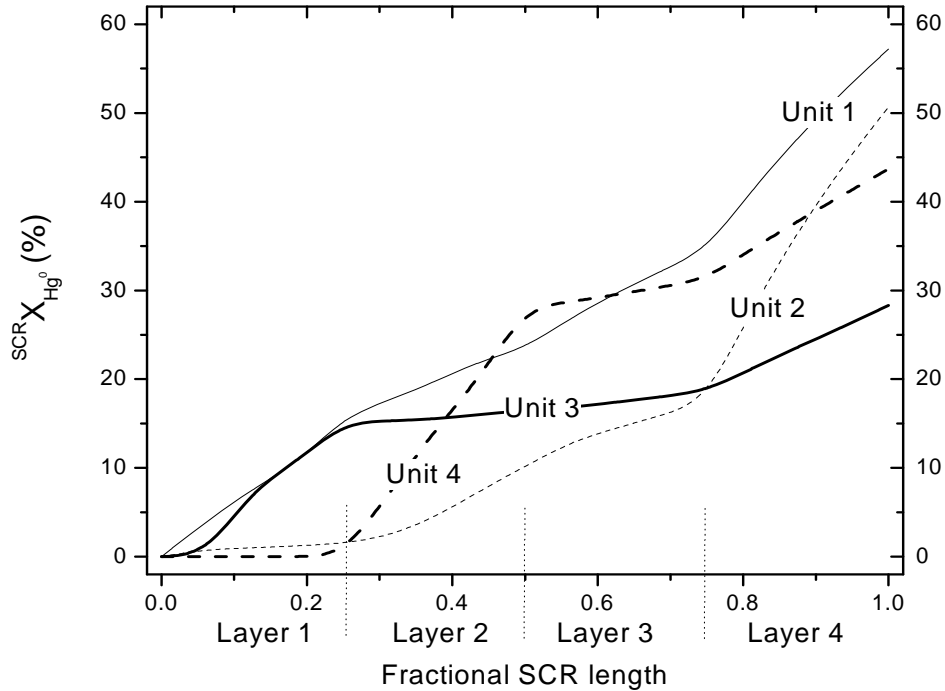

fresh and the deactivated catalysts are the same due to the overdesign of the SCR with respect to NO reduction, the $^{SCR}X_{Hg0}$ values are 85.4 % for fresh catalyst, and 57 and 79 % for deactivation of Types I and II, respectively. The substantial difference for these two deactivation scenarios highlights the importance of understanding the different catalyst poisons and their associated deactivation mechanisms.

The effect of NH_3 inhibition is also evident in the comparison of Hg^0 oxidation across layers 1 and 4 of Units 1 and 4. The two end layers at each of the respective units have the same ages and activity ratios under the extremes in NH_3 concentrations. At both units, $^IX_{Hg0}$–values are greater by almost 20 % across layer 4 than across layer 1. The implication is that a fresh catalyst layer should be added towards the end of the SCR to obtain the greatest benefit for Hg^0 oxidation under the weakest inhibitory effect of NH_3. But the activities of the preceding layers play an important role, and we find that better performance can sometimes be achieved by placing the freshest layer at intermediate positions.

The predictions for Type II deactivation follow these same trends except that the extents of Hg^0 oxidation are consistently greater, as demonstrated in Fig. 2.

We next examine the correlation between the predicted Hg^0 oxidation and the flue gas HCl concentrations across the nine power plants in this study, where only one SCR is

9

Figure 4. The extents of Hg^0 oxidation (hatched bars) for fresh catalyst (top panel) and Type I deactivation (bottom panel) in order of increasing HCl concentrations (□). The number of catalyst layers (▲) is plotted

on the right y-axis.
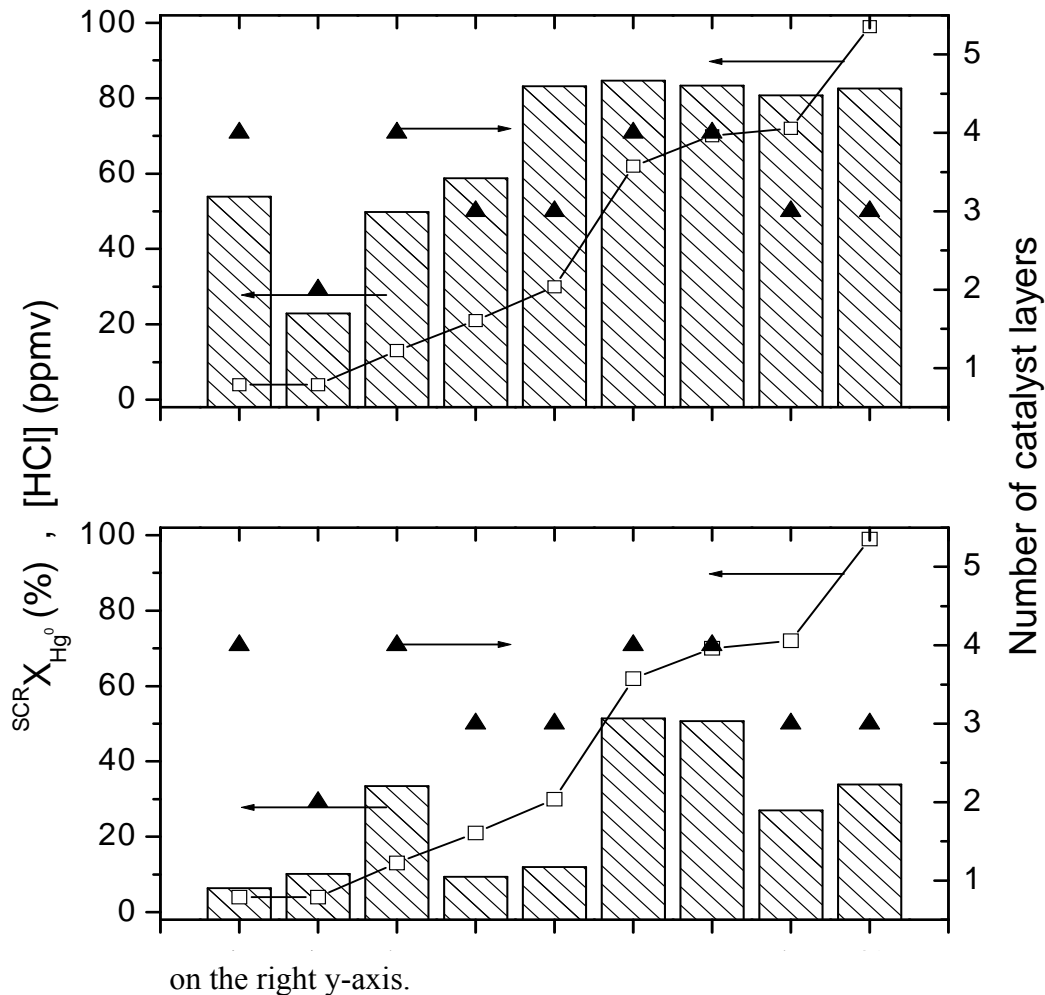
included from the plants with multiple SCRs. In this comparison, the SCRs have layers with very different design specifications and ages, and widely variable operating conditions. Figure 4 shows the predicted Hg^0 oxidation for fresh catalysts and catalysts subject to Type I deactivation arranged in order of increasing Cl concentration. The HCl concentrations and the numbers of layers are also shown.   The general trends in these predictions are the same for Type II deactivation.

Consequently, both types of deactivation completely disrupt the apparent dependence on Cl levels. Except for one unit, the fresh catalyst layers exhibit the expected Cl dependence, which is nominally first-order (or directly proportional) through moderate HCl concentrations (to about 30 ppm), but then saturates to a negligible dependence for the greatest Cl concentrations. This trend is clearly apparent in the ranked Hg^0 oxidation

performance for fresh catalysts. But the trend is thoroughly disrupted for the deactivated catalysts. Although more HCl is widely expected to give greater extents of Hg^0 oxidation, the figure demonstrates that it is not the determining factor for deactivated catalysts. For deactivated catalysts, the number of layers is much more indicative of the Hg^0 oxidation performance, in that SCRs with four layers perform better than those with three layers, with one exception whose Cl concentration is the lowest of all and whose NH_3 level is relatively high, and whose layers are much older. Similarly, the SCRs with three layers outperform the two layer units, with one exception. Notwithstanding the predominant role for the number of layers, the expected Cl dependence is apparent among SCRs with the same number of layers; i. e., Hg^0 oxidation is greater for progressively greater Cl concentrations among SCRs with the same number of layers, even for an assortment of catalyst design specifications and operating conditions.

DISCUSSION

NEA's expanded version of the SCR Catalyst Model has simulated every SCR in the SC fleet for fresh catalysts and under two deactivation scenarios. An SCR may contain up to five layers, and each layer is specified independently, so that all combinations of manufacturer, design specifications, and extents of deactivation are permitted among the layers. This generalization is obviously essential to practical applications, because the SCRs in any large commercial fleet contains layers with different catalyst properties; even when the properties are the same or similar, extents of deactivation are almost always different. Among the important factors that determine SCR performance, the only one that is not included is flue gas maldistribution.

In lieu of interlayer data to characterize deactivation, we used manufacturer's deactivation histories and the reported operating hours for each layer to estimate a diminished activity ratio. In turn, the activity ratios specified NO_X conversion across each layer, and the conversions were then reproduced under two deactivation scenarios by the SCR Catalyst Model. The premise for Type I deactivation is simultaneous destruction of the sites for the chemistries involving both NO/NH_3 species and HCl/Hg^0 species, as happens with pore plugging. Accordingly, the NO reduction reactivity was adjusted to match the NO_X conversion, then the same proportionate reduction was applied to the Hg^0 oxidation reactivity. The premise for Type II deactivation is destruction of the sites for NO/NH_3 chemistry without any disruption of HCl/Hg^0 chemistry, as can happen with chemical poisons such as As and P. So only the NO reduction reactivity was reduced to match the specified NO_X conversion. These two deactivation types provide useful bounds on the ways that deactivation affects Hg^0 conversion, although even more drastic disruptions could be implemented by extending the reactivity adjustments to the adsorption equilibria for NH_3 and/or halogen species.

Both types of deactivation slow the rate of NO reduction, which sustains greater NH_3 concentrations deeper into the monolith. Since NH_3 adsorption inhibits the adsorption of halogen species, the persistence of NH_3 disrupts Hg^0 conversion. In addition, the reduction in the Hg^0 oxidation reactivity compounds the stronger NH_3 inhibition, but only under Type I deactivation. The predicted impact of deactivation on Hg^0 conversion was

significant for every SCR in the fleet under both deactivation types. For Type I deactivation, the relative reductions vary from about 33 to 92 %, and the median reduction is 67 %. For Type II deactivation, the relative reductions vary from about 6 to 53 %, and the median reduction is 25 %.

Whereas our primary goal in this stage of the project was to expand the analysis to cover SC's entire fleet, a few parametric sensitivity studies started to unravel the factors that determine Hg^0 conversions in the field. Our most striking finding is that both types of deactivation completely disrupt the apparent dependence on Cl levels. Except for one SCR, the fresh catalysts exhibit the expected Cl dependence, which is nominally first-order through HCl concentrations to about 30 ppm, but then saturates to a negligible dependence for the greatest Cl concentrations. But the trend is thoroughly disrupted for the deactivated catalysts. For deactivated catalysts, the number of layers is much more indicative of the Hg^0 oxidation performance, in that SCRs with four layers perform better than those with three layers, etc. The new conclusion is that Hg^0 oxidation is greater for progressively greater Cl concentration among SCRs with the same number of layers, even for an assortment of catalyst design specifications and operating conditions.

ACKNOWLEDGEMENT

REFERENCES

1. Chu, P., Laudal, D., Brickett, L., and Lee, C. W., "Power plant evaluation of the effect of SCR technology on mercury," Proc. U. S. EPA-DoE-EPRI Combined Power Plant Air Pollutant Control Symp.: The MEGA Symp., 2003, Washington, DC, May 19-22.
2. Niksa, S. and Freeman Sibley, A., "Relatingcatalystproperties to the multipollutant performance of full-scale SCR systems", Ind. Eng. Chem. Res., 49, 6332-41, 2010.
3. Niksa, S. and Freeman Sibley, A., "Relatingcatalystproperties to the multipollutant performance of full-scale SCR systems," Int. Conf. on Air Quality VII, UND EERC, Arlington, VA, Sep. 2009.
4. Niksa,S. and Freeman Sibley, A.,"Relatingcatalystproperties to the multipollutant performance of full-scale SCR systems," EPRI-DOE-EPA-A&WMA Combined Utility Air Pollution Control Symposium: The MEGA Symp., 2010, Baltimore, MD, Aug. 30 – Sep. 2.
5. Niksa, S. and Fujiwara, N., "A predictivemechanism for mercuryoxidation on SCR catalystsundercoal-derived flue gas," J. AWMA, **2005**, 56, 1866-75.
6. Kamata, H., Ueno, S.-I., Naito, T., and Yukimura, A., "Mercuryoxidation over the $V_2O_5(WO_3)/TiO_2$ SCR catalyst, " Ind. Eng. Chem. Res., **2008**, 47, 8136-41.